



Short communication

A facile room temperature chemical route to Pt nanocube/carbon nanotube heterostructures with enhanced electrocatalysis

Qian Wang, Baoyou Geng*, Bo Tao

College of Chemistry and Materials Science, Anhui Key Laboratory of Functional Molecular Solids, Anhui Laboratory of Molecular-Based Materials, Anhui Normal University, No. 1 Beijing East Road, Wuhu 241000, PR China

ARTICLE INFO

Article history:

Received 14 April 2010

Received in revised form 11 June 2010

Accepted 11 June 2010

Available online 23 June 2010

Keywords:

Pt/carbon nanotube

Heterostructures

Nanostructures

Fuel cell

Catalyst

ABSTRACT

The fascinating heterostructure of carbon nanotube-supported metal nanoparticles continues to attract interest for developing electrocatalysts for energy sciences. Here, we report the fabrication of noble metal nanocubes carbon nanotube nanocomposites through an electroless deposition route. The as-synthesized carbon nanotubes-supported Pt nanocubes with high active and selective {100} surfaces display excellent electrocatalytic activities towards the oxygen reduction reaction, which can/will replace current/state of the art cathode catalysts in fuel cells, and thereby improve the catalytic performance and utilization efficiency. The methodology presented here could be further extended to fabricate other one-dimensional materials/noble metal nanostructures.

© 2010 Elsevier B.V. All rights reserved.

1. Introduction

In recent years, noble metallic nanostructures have been widely used as electrocatalysts in fuel cell [1]. Especially, Pt and its alloy nanostructures have been found as the key electrocatalyst in polymer electrolyte membrane fuel cells (PEMFCs) and direct methanol fuel cells (DMFCs) [2]. Previous research has demonstrated that the catalytic activity of Pt nanostructures depends highly on their morphology and sizes, which is crucial for their applications in the field of electrocatalysis for fuel cells [3]. However, before achieving their commercial application in fuel cells, some major problems must be resolved, such as low electrochemical active surface area and low utilization efficiency of cathode catalysts [4].

In order to improve catalytic efficiency, and reduce cost, different kinds of carbon materials, such as black carbon (BC), carbon nanotubes (CNTs), and graphene have been used as supports to disperse noble metallic nanoparticles [5]. In particular, CNTs are an important support which have been extensively used as support materials for dispersing noble metal nanoparticles [6]. However, most of the previous studies mainly involved spherical noble metal nanoparticles or nanoparticles with an undetermined shape. Current investigations indicate that the reactivity and selectivity of noble metal nanoparticles can be tailored not only by controlling the size of the nanoparticles, but also by adjusting their morphol-

ogy, which will determine the structure of crystallographic facets exposed on the surfaces of a nanocrystal and impact their potential applications [7].

Very recently, fabrication of noble metallic nanocrystals with specific shapes has attracted extensive interests because of their unique optical, magnetic, and catalytic properties and their potential applications in many fields, such as biodiagnostics, plasmonics, catalysis, and so on [8–12]. As a key catalyst for fuel cells, the morphologies of Pt nanostructures have received increasing attention [13]. Many researches have found that specific shapes of Pt nanostructures exhibit much superior catalytic action [14,7f]. Therefore, cubic Pt-based nanoparticles have drawn much attention owing to their unique structure and surface properties, as well as excellent electrocatalytic activities [15]. However, Pt nanocubes are general fabricated through a complicated process and the complex between Pt nanoparticles and supports often leads to the unwanted aggregation of the nanoparticles. Therefore, the fabrication of Pt nanocubes/CNTs composite catalysts with high dispersions is still a challenge.

In this paper, we report a facile room temperature wet chemical approach toward single-crystal platinum nanocubes/CNTs heterostructures with high dispersions. The as-synthesized CNT-supported Pt nanocubes with high active and selective {100} surfaces [16] display excellent electrocatalytic activities towards the oxygen reduction reaction (ORR) [17], which will replace current cathode materials in fuel cells, and thereby improve the catalytic performance and utilization efficiency. The obtained material is a promising fuel cell electrode material.

* Corresponding author. Tel.: +86 553 5991196; fax: +86 553 3869303.

E-mail address: bygeng@mail.ahnu.edu.cn (B. Geng).

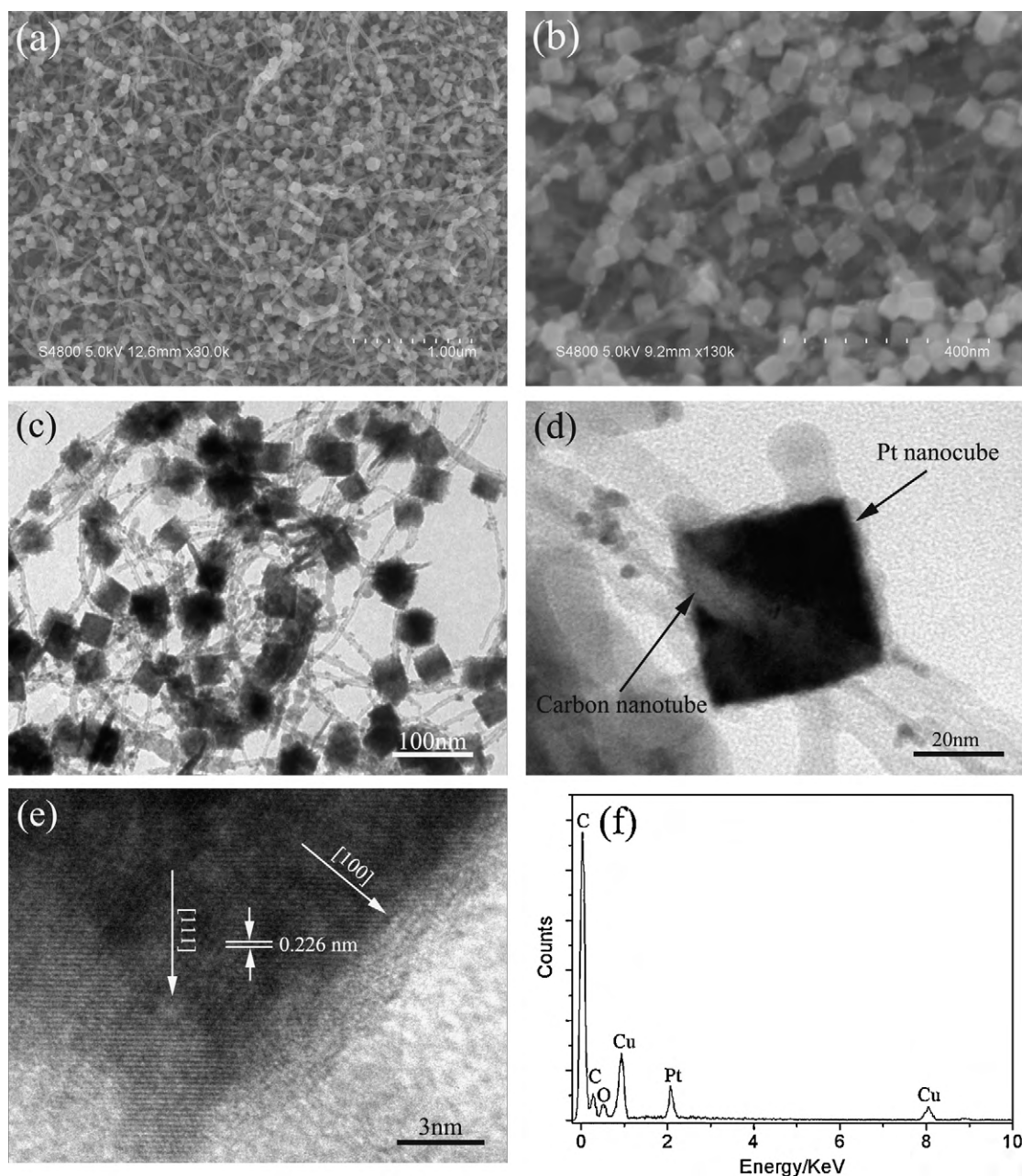


Fig. 1. Structure characterization of the Pt nanocube/CNT heterostructures. (a and b) Typical SEM images of Pt/CNT hybrids at different magnifications. (c and d) TEM images of Pt/CNT heterostructures. (e) HRTEM image of the Pt nanocube. (f) EDX spectrum of the products.

2. Experimental

2.1. Chemicals

Multi-walled carbon nanotubes (MWNTs, CVD method, purity >95%) were purchased from Nanotech Port. Co. Ltd. (Shenzhen, PR China) and were used as received. $\text{H}_2\text{PtCl}_6 \cdot 6\text{H}_2\text{O}$ was purchased from the Shanghai Chemical Factory (Shanghai, PR China). Other chemicals were of analytical grade and were used without further purification. Water used throughout all experiments was purified with the Millipore system.

2.2. Nanotube processing

Polymer wrapping was performed by means of a variation of the method reported by O'Connell et al. [18]. A controlled amount of

MWNTs was dispersed in a 0.5 wt% aqueous solution of an anionic polyelectrolyte, polystyrene sulfonate (PSS, $M_w = 70,000$), to a concentration of 150 mg L^{-1} by a combination of strong stirring and sonicating to ensure that well-dispersed individual MWNTs were present in the dispersion. Excess PSS was removed by three centrifugation/redispersion cycles.

2.3. Preparation of CNTs/metal heterostructures

The dispersion of polymer-wrapped MWNTs was then spun-coated onto a copper foil (25 mm^2) and subsequently immersed into an aqueous solution of $3 \text{ mM H}_2\text{PtCl}_6$ in the presence of 1.25 mM CoCl_2 at room temperature. The copper foil was taken out after reacting with solution for 1 min and thoroughly washed with distilled water. The size and loading control of metal nanoparticles were realized by changing the concentration of the metal salt ions and the reaction time.

2.4. Characterization

SEM imaging was performed on a Hitachi S-4800 field emission scanning electron microscope. TEM images were obtained using a transmission electron microscope (JEM 2010 F). An energy-dispersive X-ray spectroscopic (EDS) detecting unit was used for the element analysis. Cyclic voltammetry (CV) scans were recorded using a CHI660 electrochemical workstation (Shanghai, China) with a conventional three-electrode system composed of a platinum wire as counter electrode, KCl-saturated Ag/AgCl as reference electrode, and a glass-carbon (GC) electrode (3 mm diameter) as working electrode. All potentials reported here refer to the Ag/AgCl (sat. KCl) reference electrode. Cyclic voltammetric experiments were performed in a quiescent solution.

2.5. Electrocatalytic experiment

The GC electrode (3 mm) was loaded with Pt/CNT (3 μL). Electrocatalytic oxygen reduction measurements were carried out in a 0.5 M H_2SO_4 aqueous solution at a scan rate of 100 mV s^{-1} . For the RRDE voltammetry experiment, 10 μL (Pt loading of 40 wt%) of hybrid nanomaterial solution was dropped onto the GC electrode (3 mm) and allowed to dry at room temperature. Then, 10 μL of Nafion (0.2%) solution was placed on the surface of the Pt/CNT heterostructures-modified GC electrode.

3. Results and discussion

The Pt nanocubes/CNTs heterostructures were prepared by electrodeless deposition technology. The main procedure of our experiments was illustrated in Supporting Information Scheme S1.

The morphology of the obtained products is shown in Fig. 1a and b. As shown in Fig. 1a, well-dispersed and isolated Pt nanocubes are strung by the CNTs to form necklace-like nanostructures. No aggregation took place during the generation of the Pt nanocubes, indicating that homogeneous nucleation is suppressed. The high-magnification SEM image (Fig. 1b) indicates that the obtained Pt nanocubes are uniform with an average size of about 30–40 nm and the composite are formed in high yield. The corresponding TEM image (Fig. 1c) clearly displays that the CNTs are decorated by numerous Pt nanocubes. Few unsupported nanocubes could be observed in the background of TEM image, which demonstrates that Pt nanocubes have strong interaction with CNTs. Fig. 1d shows the high-magnification TEM of single Pt nanocube, which clearly exhibits that a CNT threads through the nanocube, as marked with the arrows. The high-resolution TEM (HRTEM) image (Fig. 1e) reveals the single-crystal nature of the nanocube; the lattice spac-

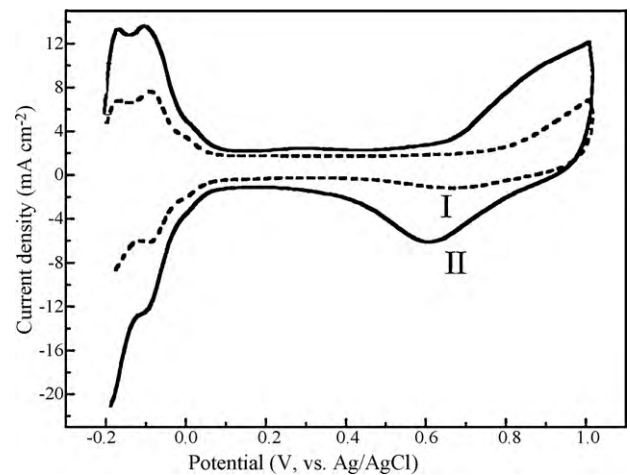


Fig. 2. Cyclic voltammograms (CVs) of (I) commercial Pt/C catalyst and (II) CNT/Pt heterostructures in 0.5 M H_2SO_4 aqueous solution saturated with nitrogen (scan rate 20 mV s^{-1}).

ing of 0.226 nm is indexed as {1 1 1} of fcc Pt, which illustrates that the as-synthesized Pt nanocubes are bounded by {1 0 0} surfaces. The presence of Pt in the product is confirmed by energy-dispersive X-ray spectroscopy (Fig. 1f).

To better understand the selective deposition of noble metal nanocubes on CNTs, the following aspects should be addressed, as shown in Supplementary Scheme S2. Firstly, salt effects (CoCl_2) increase the barrier towards homogeneous nucleation and heterogeneous nucleation becomes more favorable. Secondly, the autocatalytic growth of the particles rapidly depletes the noble metal-monomer concentration in the solutions, consequently effectively suppressing homogeneous nucleation. Therefore, a high density of uniform Pt nanocubes decorated CNTs could be obtained. We have extended this method to other noble metals and found that Au nanocube/CNT and Pd nanocube/CNT could also be fabricated with the similar conditions (see Supporting Information Fig. S2).

The electrochemical active surface (EAS) area and electrochemical performance of the Pt nanocube/CNT composites and commercial Pt/C catalyst (E-TEK) were investigated, with metal loadings of 40 wt%. Fig. 2 shows a cyclic voltammogram of (I) commercial Pt/C catalyst-modified glass-carbon electrode and (II) CNT/Pt hybrids-modified glass-carbon electrode in 0.5 M H_2SO_4 saturated by nitrogen at a scan rate of 20 mV s^{-1} . The current densities in the hydrogen adsorption/desorption and oxide formation/reduction regions of the Pt nanocube/CNT composites (Fig. 2II)

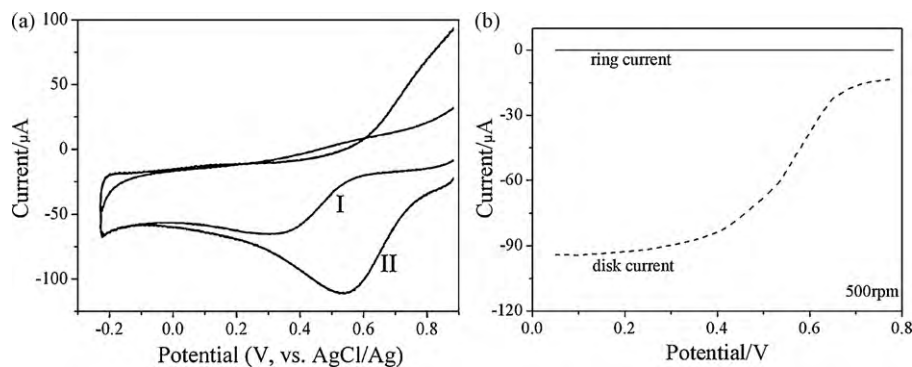


Fig. 3. Electrochemical properties of CNT/Pt nanocomposites. (a) Cyclic voltammograms (CVs) of O_2 reduction at (I) commercial Pt/C catalyst-modified glass-carbon electrode and (II) CNT/Pt heterostructures-modified glass-carbon electrode in an air-saturated 0.5 M H_2SO_4 aqueous solution (scan rate 50 mV s^{-1}). (b) Current-potential curves for the reduction of O_2 at a rotating platinum ring GC electrode with CNT/Pt composition adsorbed on the disk electrode in an air-saturated 0.5 M H_2SO_4 solution. The potential of the ring electrode was maintained at 1.0V (rotation rate 500 rpm, scan rate 50 mV s^{-1}).

are much larger than that of commercial Pt/C catalyst (Fig. 2I), indicating a larger area of electrochemical activity for Pt nanocube/CNT composites, which is believed to be a result of the presence of well-dispersed, Pt nanocubes and the unique structure and electric properties of MWNTs.

Activity for the ORR is an important criterion in the assessment of novel catalysts for fuel cells. The electrocatalytic performances of the catalysts for the ORR were tested by CV, as shown in Fig. 3. Fig. 3a shows typical CVs of oxygen reduction at (I) commercial Pt/C (0.5 mg Pt cm⁻², E-TEK) catalyst-modified glass-carbon electrode and (II) CNT/Pt hybrids-modified glass-carbon electrode in a 0.5 M H₂SO₄ aqueous solution in the presence of air. Compared the obtained CVs, we can clearly find that the CNT/Pt hybrids-modified glass-carbon electrode exhibits a more positive potential (about 0.55 V) and higher current for dioxygen reduction than that of the commercial Pt/C catalyst-modified glass-carbon electrode. The results reveal that the obtained Pt/CNT heterostructures-modified electrode shows good electrocatalytic activity toward ORR. Most importantly, we also find that the reduction potential (0.55 V) for the Pt nanocube/CNT electrode possesses significantly more positive than those of previously reported catalysts, such as CNT/Pt nanocubes (6.2 nm) [19], CNT/Pt nanoparticles [20], core/shell Pt/C nanoparticles embedded in mesoporous carbon [21], and 6 nm Pt NPs [22]. The superiority of the catalyst may be attributed to the special cubic morphology of Pt nanoparticles and presence of the Pt nanocube and CNT heterostructure.

To better understand the superiority of the obtained materials, we studied its catalytic activity by rotating disk electrode (RDE) and rotating ring disk electrode (RRDE) experiments. In this experiment, we scanned the disk potential from +0.75 V to 0.15 V while ring potential was kept at +1.0 V during this experiment. The typical ring current and disk current responses at 500 rpm (see Fig. 3b) clearly shows a large disk current is obtained whereas almost no ring current is observed, thereby which illustrates that the as-prepared Pt/CNT heterostructures-modified electrode reduces O₂ predominantly by a four-electron process to H₂O. The collection efficiency (*N*) of the ring electrode obtained by reducing ferricyanide at a disk electrode was 0.139. Here, from Fig. 3b, we also calculated the number of electrons (*n*) closed to 4 (3.96) involved based on RRDE data through the equation: $n = 4I_{\text{disk}} / (I_{\text{disk}} + I_{\text{ring}}/N)$, where *I*_{disk} and *I*_{ring} are the limiting currents for disk and ring electrodes, respectively [23,24]. The above results indicate that most oxygen molecules participating in the reaction are reduced to water. These features make the obtained catalyst attractive for future application in fuel cells.

4. Conclusion

In summary, we have fabricated Pt nanocube/CNT heterostructures through a simple, efficient, and economical electrodeless deposition processes. The metallic Pt nanocubes are well-dispersed on the surface of CNTs. The in situ fabrication of Pt nanocubes on CNTs eliminates the need for complicated sorting, washing, and post processing required for most CNT-electrode immobilization schemes. This method could also be used to prepare heterostructures composed of other noble metals and CNTs. The obtained Pt nanocube/CNT heterostructures exhibit good electric conductivity, high electroactive surface area, and high electrocatalytic activity toward the reduction of O₂. The obtained Pt nanocube/CNT nanocomposites could be a promising heterogeneous catalyst or fuel cell electrode material.

Acknowledgements

This work was supported by the National Natural Science Foundation of China (20671003, 20971003), the Key Project of Chinese Ministry of Education (209060), Science and Technological Fund of Anhui Province for Outstanding Youth (10040606Y32), the Education Department of Anhui Province (2006KJ006TD) and the Program for Innovative Research Team in Anhui Normal University.

Appendix A. Supplementary data

Supplementary data associated with this article can be found, in the online version, at doi:10.1016/j.jpowsour.2010.06.035.

References

- [1] (a) K.Y. Chan, J. Ding, J. Ren, S. Cheng, K.Y. Tsang, J. Mater. Chem. 14 (2004) 505; (b) D. Zhao, B.Q. Xu, Angew. Chem. Int. Ed. 45 (2006) 4955; (c) N. Hoshi, K. Kida, M. Nakamura, M. Nakada, K. Osada, J. Phys. Chem. B 110 (2006) 12480.
- [2] (a) T.E. Mallouk, Nature 343 (1990) 515; (b) B.C.H. Steele, A. Heinzl, Nature 414 (2001) 345; (c) D.R. Rolison, Science 299 (2003) 1698; (d) M.H. Shao, K. Sasaki, R.R. Adzic, J. Am. Chem. Soc. 128 (2006) 3526; (e) I. Dabo, A. Wieckowski, N. Marzari, J. Am. Chem. Soc. 129 (2007) 11045; (f) P. Ferrin, M. Mavrikakis, J. Am. Chem. Soc. 131 (2009) 14381; (g) B. Lim, M.J. Jiang, P.H.C. Camargo, E.C. Cho, J. Tao, X.M. Lu, Y.M. Zhu, Y.N. Xia, Science 324 (2009) 1302; (h) J.P. Wang, R.M. Asmussen, B. Adams, D.F. Thomas, A.C. Chen, Chem. Mater. 21 (2009) 1716.
- [3] (a) J. Chen, T. Herricks, Y.N. Xia, Angew. Chem. 117 (2005) 2645; (b) J. Chen, T. Herricks, Y.N. Xia, Angew. Chem. Int. Ed. 44 (2005) 2589; (c) H. Lee, S.E. Habas, S. Kweskin, D. Butcher, G.A. Somorjai, P. Yang, Angew. Chem. 118 (2006) 7988; (d) H. Lee, S.E. Habas, S. Kweskin, D. Butcher, G.A. Somorjai, P. Yang, Angew. Chem. Int. Ed. 45 (2006) 7824.
- [4] (a) F.R. Service, Science 315 (2007) 172; (b) V.R. Stamenkovic, B. Fowler, B.S. Mun, G.F. Wang, P.N. Ross, C.A. Lucas, N.M. Markovic, Science 315 (2007) 493; (c) V.R. Stamenkovic, B.S. Mun, M. Arenz, K.J.J. Mayrhofer, C.A. Lucas, G.F. Wang, P.N. Ross, N.M. Markovic, Nat. Mater. 6 (2007) 241; (d) Z.M. Peng, H. Yang, Nano Today 4 (2009) 143; (e) H.A. Gasteiger, S.S. Kocha, B. Sompalli, F.T. Wagner, Appl. Catal. B 56 (2005) 9.
- [5] (a) S. Hrapovic, Y.L. Liu, K.B. Male, J.H.T. Luong, Anal. Chem. 76 (2004) 1083; (b) K. Zhao, S.Q. Zhuang, Z. Chang, H.Y. Song, L.M. Dai, P.G. He, Y.Z. Fang, Electroanal. 19 (2007) 1069; (c) Y.C. Xing, J. Phys. Chem. B 108 (2004) 19255; (d) Y.H. Lin, X.L. Cui, C. Yen, C.M. Wai, J. Phys. Chem. B 109 (2005) 14410; (e) M. Sanles-Sobrido, M.A. Correa-Duarte, S. Carregal-Romero, B. Rodríguez-González, R.A. Álvarez-Puebla, P. Hervés, L.M. Liz-Marzán, Chem. Mater. 21 (2009) 1531; (f) S.J. Guo, S.J. Dong, E.K. Wang, ACS Nano 4 (2010) 547.
- [6] (a) K. Jiang, A. Eitan, L.S. Schadler, P.M. Ajayan, R.W. Siegel, N. Grobert, M. Mayne, M. Reyes-Reyes, H. Terrones, M. Terrones, Nano Lett. 3 (2003) 275; (b) Y. Zhang, H. Dai, Appl. Phys. Lett. 77 (2000) 3015; (c) B. Xue, P. Chen, Q. Hong, J. Lin, K. Tan, J. Mater. Chem. 11 (2001) 2378; (d) J. Li, M. Moskovits, T. Haslett, Chem. Mater. 10 (1998) 1963; (e) R. Azamian, K. Coleman, J. Davis, N. Hanson, M. Green, Chem. Commun. 366 (2002); (f) A.V. Ellis, K. Vijayamohan, R. Goswami, N. Chakrapani, L.S. Ramanathan, P.M. Ajayan, G. Ramanath, Nano Lett. 3 (2003) 279.
- [7] (a) J.G. Ulan, W.F. Maier, J. Org. Chem. 52 (1987) 3132; (b) R. Narayanan, M.A. El-Sayed, Nano Lett. 4 (2004) 1343; (c) A. Komakov, D.O. Kelnov, Y. Lilach, S. Stemmer, M. Moskovits, Nano Lett. 5 (2005) 667; (d) F. Mirkhalaf, J. Paprotny, D.J. Schiffrin, J. Am. Chem. Soc. 128 (2006) 7400; (e) S.H. Sun, G.X. Zhang, D.S. Geng, Y.G. Chen, M.N. Banis, R.Y. Li, M. Cai, X.L. Sun, Chem. Eur. J. 16 (2010) 829.
- [8] (a) C. Burda, X.B. Chen, R. Narayanan, M.A. El-Sayed, Chem. Rev. 105 (2005) 1025; (b) Y.N. Xia, N.J. Halas, Mater. Res. Bull. 30 (2005) 338; (c) L.M. Liz-Marzán, Langmuir 22 (2006) 32; (d) M.P. Pileni, J. Phys. Chem. C 111 (2007) 9019.
- [9] (a) B.J. Wiley, S.H. Im, Z.Y. Li, J. McLellan, A. Siekkinen, Y.N. Xia, J. Phys. Chem. B 110 (2006) 15666; (b) C.J. Murphy, T.K. Sau, A.M. Gole, C.J. Orendorff, J.X. Gao, L.F. Gou, S.E. Hunyadi, T. Li, J. Phys. Chem. B 109 (2005) 13857; (c) H. Lee, S.E. Habas, S. Kweskin, D. Butcher, G.A. Somorjai, P.D. Yang, Angew. Chem. Int. Ed. 46 (2006) 7988;

- (d) K.M. Bratlie, H. Lee, K. Komvopoulos, P.D. Yang, G.A. Somorjai, *Nano Lett.* 7 (2007) 3097.
- [10] (a) M.S. Chen, D. Kumar, C.W. Yi, D.W. Goodman, *Science* 310 (2005) 291;
(b) N.L. Rosi, C.A. Mirkin, *Chem. Rev.* 105 (2005) 1547;
(c) A.R. Tao, P. Sinsermsuksakul, P.D. Yang, *Nat. Nanotechnol.* 2 (2007) 435.
- [11] (a) Z.Q. Tian, B. Ren, *Annu. Rev. Phys. Chem.* 55 (2004) 197;
(b) C.J. Orendorff, A. Gole, T.K. Sau, C.J. Murphy, *Anal. Chem.* 77 (2005) 3261;
(c) Z.Q. Tian, B. Ren, J.F. Li, Z.L. Yang, *Chem. Commun.* 34 (2007) 3514.
- [12] F.R. Fan, D.Y. Liu, Y.F. Wu, S. Duan, Z.X. Xie, Z.Y. Jiang, Z.Q. Tian, *J. Am. Chem. Soc.* 130 (2008) 6949.
- [13] (a) Z.W. Chen, M. Waje, W.Z. Li, Y.S. Yan, *Angew. Chem. Int. Ed.* 46 (2007) 4060;
(b) S.J. Jiang, Y.W. Ma, G.Q. Jian, H.S. Tao, X.Z. Wang, Y.N. Fan, Y.N. Lu, Z. Hu, Y. Chen, *Adv. Mater.* 21 (2009) 4953;
(c) F. Ksar, G. Surendran, L. Ramos, B. Keita, L. Nadjo, E. Prouzet, P. Beaunier, A. Hagège, F. Audonnet, H. Remita, *Chem. Mater.* 21 (2009) 1612.
- [14] Z.Y. Zhou, Z.Z. Huang, D.J. Chen, Q. Wang, N. Tian, S.G. Sun, *Angew. Chem. Int. Ed.* 49 (2010) 411.
- [15] D. Xu, S. Bliznakov, Z.P. Liu, J.Y. Fang, N. Dimitrov, *Angew. Chem. Int. Ed.* 49 (2010) 1282.
- [16] C.X. Ji, P.C. Searson, *Appl. Phys. Lett.* 81 (2002) 4437.
- [17] R.J. Davis, E.G. Derouane, *Nature* 349 (1991) 313.
- [18] M.J. O'Connell, P. Boul, L.M. Ericson, C. Huffman, Y. Wang, E. Haroz, C. Kuper, J. Tour, K.D. Ausman, R.E. Smalley, *Chem. Phys. Lett.* 342 (2001) 265.
- [19] Y. Wen, X.L. Wang, C. Yang, X.R. Yang, *Adv. Mater.* 20 (2008) 2579.
- [20] X.G. Hu, T. Wang, L. Wang, S.J. Guo, S.J. Dong, *Langmuir* 23 (2007) 6352.
- [21] Z. Wen, J. Liu, J. Li, *Adv. Mater.* 20 (2008) 743.
- [22] S.J. Guo, S.J. Dong, E.K. Wang, *Chem. Eur. J.* 14 (2008) 4689.
- [23] (a) Y.D. Jin, Y. Shen, S.J. Dong, *J. Phys. Chem. B* 108 (2004) 8142S;
(b) J. Guo, J.F. Zhai, Y.X. Fang, S.J. Dong, E.K. Wang, *Chem. Asian J.* 3 (2008) 1156.
- [24] Z. Wei, U.S. Ali, Y.T. Emily, M.S. Timothy, *Chem. Mater.* 21 (2009) 3234.